Ordering at Two Length Scales in Comb−Coil Diblock Copolymers Consisting of Only Two Different Monomers

Rikkert J. Nap and Gerrit ten Brinke*

Department of Polymer Chemistry and Materials Science Centre, University of Groningen, Nijenborgh 4, 9747 AG Groningen, The Netherlands

Received March 26, 2001; Revised Manuscript Received September 11, 2001

ABSTRACT: The microphase-separated morphology of a melt of a specific class of comb−coil diblock copolymers, consisting of an AB comb block and a linear homopolymer A block, is analyzed in the weak segregation limit. On increasing the length of the homopolymer A block, the systems go through a characteristic series of structural transitions. Starting from the pure comb copolymer, the first series of structures involve a short length scale followed by structures involving a large length scale. A maximum of two critical points exists. Furthermore, in the two parameter space characterizing the comb−coil diblock copolymer molecules considered, a nontrivial bifurcation point exists beyond which the structure factor can have two maxima (two correlation hole peaks).

I. Introduction

Diblock copolymer melts usually microphase separate with *one* characteristic length. However, if more than two monomer types are involved, microphase separation frequently occurs at more than one length scale.[1−7] Several examples that are of direct interest for the present paper can be found in the experimental work of Ikkala and Ten Brinke and co-workers.[4−6] There, comb−coil diblock copolymers are investigated consisting of a poly(4-vinylpyridine)-*block*-polystyrene (P4VP-*b*-PS) diblock copolymer with side chains (e.g., pentadecylphenol, PDP) attached by hydrogen bonds to the P4VP block. The resulting comb−coil diblock copolymers show typical two length scale structure-inside-structure morphologies. The PS blocks microphase separate from the P4VP(PDP) blocks, giving rise to the well-known classical morphologies depending on the volume fraction of either block. This structure corresponds to the large length scale ordering, and the order−disorder transition temperature is, if present at all, very high. Inside the P4VP(PDP) domains an additional short length scale lamellar ordering takes place characterized by an easily accessible (ca. 60 °C) order−disorder transition.

Still, two length scale ordering is not restricted to block copolymers involving three or more chemically different monomers. To demonstrate and analyze this, we studied in ref 8 the structure factor of a block copolymer consisting of a linear homopolymer block of A monomers linked to a comb copolymer block with a backbone of the same kind of A monomers and side chains consisting of B monomers. (An experimental example can be found in refs 9 and 10.) For convenience, to reduce the number of free parameters, the discussion was restricted to side chains having a length equal to the backbone length between two consecutive side chains (see Figure 1). Because of the architecture of the molecule, microphase separation can in principle occur at two different length scales, either "inside" the AB comb block or "between" the linear A block and the AB comb block (see Figure 2). In the latter case the behavior resembles that of a diblock copolymer, where one block is the homopolymer *A* block and the other block the AB comb block.

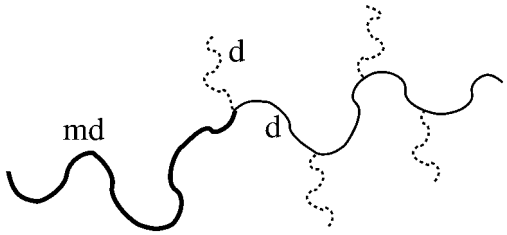

Figure 1. Model of the comb−coil diblock copolymer molecule studied. Note: for clarity, the homopolymer block is indicated with a thicker line than the backbone of the comb block. In this study both are assumed to be chemically identical. The cartoon corresponds to number of branch points $n_t = 4$, asymmetry parameter $t = 0$, and one side chain per branch point $\alpha = 1$. The length of the side chains and length of the backbone between two successive side chains equal d. The length of the homopolymer block equals md, $m \in \mathbf{R}$.

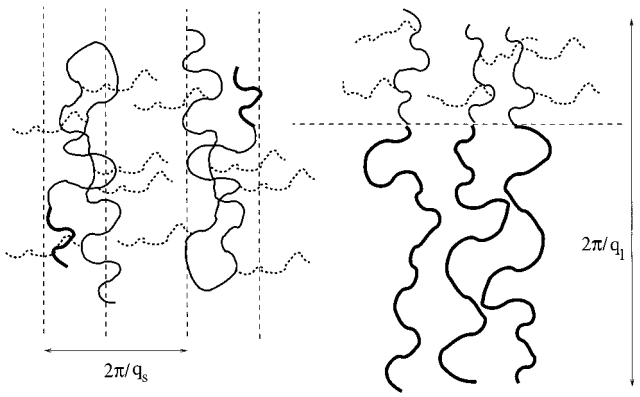

Figure 2. Illustration of the two ways in which the system can microphase separate.

In ref 8 the analysis of the structure factor of this system was presented, and the main result was summarized in the form of a so-called classification diagram. In this diagram, the horizontal and vertical axes denote respectively the number of side chains and the length of the homopolymer block; the latter is expressed in units corresponding to the side chain length. Together these two parameters uniquely determine the molecular

* To whom correspondence should be addressed.

10.1021/ma010519v CCC: $22.00
Published on Web 01/04/2002

structure for the specific class of comb−coil diblock copolymers considered, i.e., length of side chains equal to length of backbone between consecutive side chains. The position and the value of the absolute minimum of the inverse structure factor determine the length scale of microphase separation and the temperature at which the disordered phase becomes unstable against structure formation, i.e., the spinodal. The classification diagram presented showed which length scale was favored (absolute minimum of the inverse structure factor) and whether the inverse structure factor had one or two minima. One of the most striking features was the existence of a nontrivial bifurcation point, separating the region in the parameter space where the structure factor has only one minimum from the region where the structure factor can have two minima (two correlation hole peaks!).

In this paper we continue the analysis of the phase behavior of this class of systems by calculating the free energy up to fourth order in the weak segregation limit and constructing the corresponding phase diagrams.

The paper is organized as follows. In section 2 the system parameters are defined, in section 3 the theory is outlined, and in section 4 the results are discussed.

II. Parametrization

We consider monodisperse polymer melts of comb−coil diblock copolymers. The comb−coil diblock copolymer molecules differ from the comb copolymer by the fact that an additional A homopolymer block is linked to the AB comb copolymer block (see Figure 1).

First the parametrization of the comb block will be introduced. The phase behavior of pure AB comb copolymer melts, i.e., without the A homopolymer block, has already been discussed in several papers.[11−14] However, all of these, except for Dobrynin and Erukhimovich,[14] are restricted to the calculation of the spinodals only. Here, we adopt the notation introduced before[11] and extend it slightly by incorporating the possibility of having more than one side chain per branch point.

An AB comb copolymer molecule consists of a backbone chain of monomers of type A to which side chains consisting of monomers of type B are attached. The monomers (or segments) A and B are assumed to be of equal size. The number of backbone monomers equals N_A^b whereas the number of monomers per *one* side chain is equal to N_B. There are n_t branch points which all have the same functionality $z = \alpha + 2$. Here α is the number of side chains linked to *one* branch point. Therefore, the number of side chains equals $n_s = \alpha n_t$. The branch points are assumed to be distributed regularly along the backbone chain. The number of backbone segments between consecutive branch points is assumed to be equal to N_A^b/n_t. Obviously, the number of backbone segments before the first branch point and after the last branch point must then also add up to N_A^b/n_t. Therefore, the number of backbone segments before the first side chain and after the last side chain equals tN_A^b/n_t and $(1 - t)N_A^b/n_t$, respectively, with $t \in [0, 1]$, where t is called the asymmetry parameter.[11]

The A homopolymer block has N_A^h segments. Thus, the total number of A segments in the comb−coil molecule is $N_A = N_A^b + N_A^h$, and that of all segments is $N = N_A^b + N_A^h + n_s N_B$. With the above definitions the volume fractions are $f_A^b = N_A^b/N$, $f_A^h = N_A^h/N$, and $f_B = n_s N_B/N$. Since the melt is assumed to be incompressible, $f_A^b + f_A^h + f_B = 1$.

Together these parameters define a 6-dimensional compositional parameter space: (N_A^b, N_A^h, N_B, n_t, α, t). However, in our discussion of the comb−coil diblock copolymer melt, we will restrict this to a 3-dimensional subset by assuming $N_B = N_A^b/n_t = d$, $\alpha = 1$, and $t = 0$, unless stated otherwise. Hence, the length of the side chains is equal to the length of the backbone chain between consecutive side chains, and both will be denoted by d. For the comb block this implies an equal amount of A and B segments; $f_A^b = f_B$. Furthermore, we will also express N_A^h in terms of d by defining $N_A^h = dm$, where $m \in \mathbf{R}^+$ is a measure for the length of the homopolymer block in units of the side chain length. In terms of m and n_t the volume fraction of the homopolymer block becomes $f_A^h = m/(2n_t + m)$. Note that $N = (2n_t + m)d$. The overall volume fraction of A monomers is given by $f_A = (m + n_t)/(m + 2n_t)$. Because N can be absorbed in the interaction (Flory−Huggins) parameter χ, we effectively reduced the number of parameters to two, namely (n_t, m) or (n_t, f_A).

III. Theory

The Hamiltonian of the copolymer melt is given by ($\beta = 1/kT$)[15−18]

$$\beta H = \beta(H_0 + H_I) = \frac{3}{2a^2}\sum_{m,i}\delta_c\int_0^{N_i} ds \left(\frac{\partial \mathbf{R}_i^m(s)}{\partial s}\right)^2 + \frac{1}{2}\sum_{\alpha,\beta}\epsilon_{\alpha\beta}\int_V d^3r\ \hat{\rho}_\alpha(\mathbf{r})\,\hat{\rho}_\beta(\mathbf{r}) \quad (1)$$

The first part, H_0, the Edwards Hamiltonian,[16] accounts for the chain connectivity. It is a continuous model of a Gaussian chain where a configuration of the mth molecule is represented by a space curve, $\mathbf{R}^m(t)$. a is the effective bond length. We subdivide $\mathbf{R}^m(t)$ the total space curve in smaller space curves $\mathbf{R}_i^m(s)$. Here $\mathbf{R}_i^m(s)$ corresponds to the part of the space curve $\mathbf{R}^m(t)$ which is associated with the ith linear block in which the molecule will be divided. The variable i enumerates the number of different linear blocks. The variable s is a continuous variable whose value ranges from 0 to N_i along the contour of the ith block; N_i denotes the length of the ith block. We first enumerate the A blocks ($i \in \{1,..., n_t + 2\}$) and subsequently the B blocks ($i \in \{n_t + 3,..., n_s + n_t + 3\}$). Note that the B blocks correspond to the side chains and that the first A block, corresponding to the homopolymer block, is not present in the case of pure comb copolymers. Hence, N_i is equal to

$$N_i = \begin{cases} N_A^h & i = 1 & \text{homopolymer block} \\ tN_A^b/n_t & i = 2 & \\ N_A^b/n_t & 3 \le i \le n_t + 1 & \text{backbone of comb block} \\ (1-t)N_A^b/n_t & i = n_t + 2 & \\ N_B & n_t + 3 \le i \le n_s + n_t + 3 & \text{side chains} \end{cases} \quad (2)$$

The configuration, i.e., the whole space curve $\mathbf{R}^m(t)$ is obtained by linking the subchains $\mathbf{R}_i^m(s)$ together. This translates into the following constraint on $\mathbf{R}_i^m(s)$, represented by the function δ_c in eq 1.[15]

$$\delta_c = \prod_{i=1}^{n_t+1} \delta(\mathbf{R}_i^m(N_i) - \mathbf{R}_{i+1}^m(0)) \prod_{j=1}^{\alpha} \prod_{i=2}^{n_t+1} \delta(\mathbf{R}_i^m(N_i) - \mathbf{R}_{i+j+nt+1}^m(0)) \quad (3)$$

The second part, H_I, corresponds to the interaction Hamiltonian. The $\epsilon_{\alpha\beta}$ are the dimensionless effective interaction parameters between monomers of type α and β, where α and β denote either A or B. $\hat{\rho}_\alpha(\mathbf{r})$ is the microscopic monomer concentration of monomer type α at position $\mathbf{r}$ and is given by

$$\hat{\rho}_\alpha(\mathbf{r}) = \sum_{m,i} \sigma_\alpha^i \int_0^{N_i} \mathrm{d}s\, \delta(\mathbf{r} - \mathbf{R}_i^m(s)) \quad (4)$$

The variable σ_α^i denotes whether the ith block is of monomer type α or not.

$$\sigma_\alpha^i = \begin{cases} 1 & \text{if block } i \text{ is of type } \alpha \\ 0 & \text{otherwise} \end{cases} \quad (5)$$

On imposing incompressibility, i.e., $\hat{\rho}_A(\mathbf{r}) + \hat{\rho}_B(\mathbf{r}) = 1$, H_I can be rewritten in the more familiar form

$$H_I = -\chi \int_V \mathrm{d}^3 r\, \hat{\Psi}^2(\mathbf{r}) + C \quad (6)$$

where C is an unimportant constant and χ is the Flory−Huggins parameter defined by $\chi = (\epsilon_{AB} - {}^1/_2(\epsilon_{AA} + \epsilon_{BB}))\beta^{-1}$. $\hat{\Psi}$ represents the concentration profile and equals the deviation of the microscopic concentration of monomer A from its average value: $\Psi(\mathbf{r}) = \hat{\rho}_A(\mathbf{r}) - f_A$.

The Landau mean-field free energy corresponds to an expansion in powers of the concentration profile $\psi(\mathbf{q}) = \langle\hat{\Psi}(\mathbf{q})\rangle$:[19,20]

$$F[\psi] = \sum_{n=2}^{4} \frac{1}{n!V^n} \sum_{\mathbf{q}_1 \cdots \mathbf{q}_n} \Gamma_n(\mathbf{q}_1,...,\mathbf{q}_n)\, \psi(\mathbf{q}_1)...\psi(\mathbf{q}_n) \quad (7)$$

The coefficients of the free energy expansion and the vertex functions Γ_n can be related to the chemical single-chain correlation functions, $g_{\alpha_1 \cdots \alpha_n}(\mathbf{r}_1,...,\mathbf{r}_n)$, either by the random phase approximation or equivalently by a saddle point approximation of the free energy functional (see Appendix).[19−23]

For a more detailed discussion of the computational details of the correlations functions, we refer to the Appendix. Through minimizing eq 7 with respect to the concentration profile $\psi(\mathbf{q})$ the equilibrium free energy is obtained.

The concentration profile $\psi(\mathbf{r})$ is expanded in a set of wave functions that obey the symmetry of a given (periodic) structure.

$$\psi(\mathbf{r}) = \sum_{m=1}^{\infty} \frac{A_m}{\sqrt{n_m}} \sum_{\mathbf{Q} \in H_m} \mathrm{e}^{i(\mathbf{Q}\mathbf{r} + \phi_\mathbf{Q})}$$

$$\psi(\mathbf{q}) = \sum_{m=1}^{\infty} \frac{A_m V}{\sqrt{n_m}} \sum_{\mathbf{Q} \in H_m} \mathrm{e}^{i\phi_\mathbf{Q}} \delta(\mathbf{Q} - \mathbf{q}) \quad (8)$$

where H_m is a set of wave vectors $\mathbf{Q}$ which describes the symmetry of the structure. A_m and $\phi_\mathbf{Q}$ correspond to the amplitudes and phases of the concentration profile. m denotes the number of harmonics or shells, H_m, and n_m is half the number of vectors of the mth harmonic. Vectors belonging to the same harmonic have the same length. The amplitudes belonging to these vectors are all equal. The length of the vectors in the first harmonic is denoted by q_0. Then the length of the vectors in the higher harmonics are fixed because they are multiples of q_0 (depending on the symmetry of the phase). By the above ansatz for the concentration profile the minimization of the free energy corresponds to minimizing F with respect to A_m and q_0.

The free energy expansion eq 7 is only valid in the weak segregation limit (WSL), i.e., close to the critical point and $|\psi| \ll 1$. In the WSL the free energy is dominated by the wave vector q^*, where q^* is equal to the value of q for which $\Gamma_2(q)$ ascertains its minimum. Thus, in the WSL we can set q_0 equal to q^*.

In this paper we will restrict ourselves to the *first harmonic approximation* (FHA)[19] of the concentration profile. Because of this, only the classical structures, i.e., disordered, lamellar, hexagonal, and spherical (bcc), can be considered. The inclusion of higher harmonics is required to discuss more complex structures such as the gyroid structure. [18,24−30] Because of the complicated nature of our structure factor, including the possibility of two maxima, we decided to consider at first only the FHA.

Two important quantities are the spinodal and the critical point. The spinodal denotes the line of instability of the disordered phase, the line in phase space where the disordered phase ($\psi = 0$) becomes absolutely unstable against fluctuations. It is given by the absolute minimum of $\Gamma_2(q)$

$$\left.\frac{\partial\Gamma_2(q)}{\partial q}\right|_{q^*} = 0 \quad \text{and} \quad \left.\frac{\partial^2\Gamma_2(q)}{\partial q^2}\right|_{q^*} > 0 \quad \text{and} \quad \Gamma_2(q^*) = 0 \quad (9)$$

Note that the $\Gamma_2(q)$ is inversely proportional to the structure factor.[15]

The critical point is given by

$$\text{spinodal} \wedge \Gamma_3(q',q',q'') = 0. \quad |q'| = |q'| = |q''| = |q^*| \quad (10)$$

It is a point on the spinodal curve where also Γ_3 becomes zero. At the critical point the phase transition is continuous, i.e., with zero amplitude. Therefore, close to the critical point, the amplitude will be small, thereby ensuring the validity of the WSL.

IV. Discussion

A. Spinodals. In our previous article,[8] the spinodals of a specific class of comb−coil diblock copolymers, for which the length of the side chains equals the length of the backbone between two successive side chains, were investigated in some detail. We start the discussion here by recalling the main results, presenting them in a slightly different manner. Figure 3 shows the spinodal surface of $(\chi N)_s$ vs n_t and m corresponding to the absolute minimum of $\Gamma_2(q)$. The change of $(\chi N)_s$ as a function of m for a fixed value of n_t is in line with the change in length scale of the microphase separation, which changes from short to long as the size of the homopolymer block is increased. This fact is most clearly demonstrated by Figure 4, where $y = a^2q^2d/6$, which is a measure of the inverse length scale squared, has been plotted as a function of n_t and m.

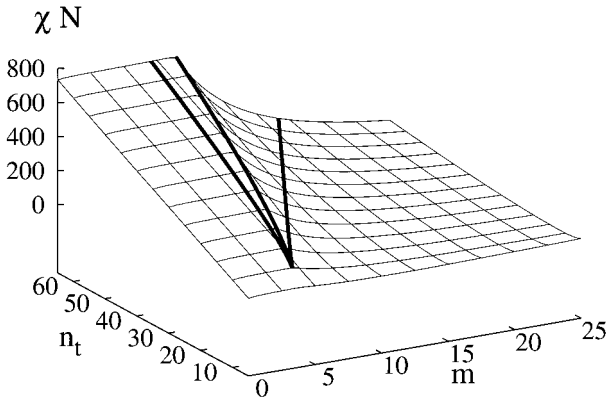

Figure 3. Spinodal value $(\chi N)_s$ for the class of comb−coil diblock copolymers defined in the text vs (n_t, m). The "outer" heavy lines on the χN surface indicate the boundary between the region where Γ_2 has one minimum and the region where Γ_2 has two minima. Along the "inner" heavy line the two minima have the same value; it separates ordering on a short length scale from ordering on a long length scale.

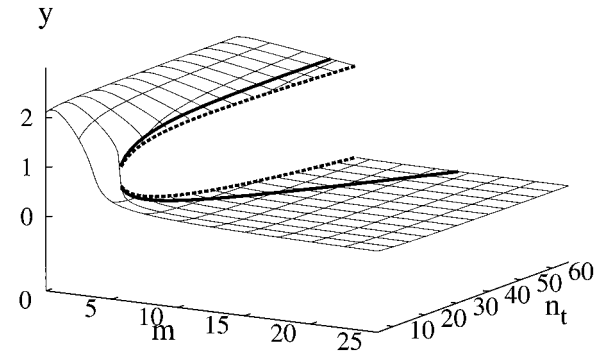

Figure 4. Spinodal value y vs (n_t, m) for the class of comb−coil diblock copolymers defined in the text., Here $y = q^{*2}R_g^2$. $R_g^2 = a^2d/6$ is the radius of gyration of a chain of length d. y is a dimensionless quantity corresponding to the inverse length scale of microphase separation. For small values of n_t, below the bifurcation point (cf. Figure 5), Γ_2 has only one minimum and y changes continuously as a function of m. For large values of n_t, above the bifurcation point, y changes discontinuously from large y (small length scale) to small y (large length scale). Here Γ_2 has two minima and the absolute minimum "jumps" from the small to the large length scale. The heavy solid lines delineate the region in which Γ_2 has two minima. Along the heavy dashed lines both minima of Γ_2 have the same value, and these lines therefore correspond to a sudden change in length scale.

A more detailed analysis[8] shows that $\Gamma_2(q)$ can have either one minimum, which in turn might correspond to either the short or the long length scale, or two minima, corresponding to the two length scales. In the latter case either the short or the long length scale corresponds to the absolute minimum of $\Gamma_2(q)$, or potentially, even more interesting, both minima have the same value. In Figures 3 and 4 the heavy lines drawn on the surfaces indicate the boundaries between the region where $\Gamma_2(q)$ has two minima and the region where $\Gamma_2(q)$ has one minimum. The line where the values of both minima are equal is also indicated. The most striking observation is the existence of a bifurcation point in the (n_t, m) parameter space. For $n_t < 10$ or $m < 4.8$ microphase separation is only possible at one length scale; i.e., $\Gamma_2(q)$ has a single minimum. Above the bifurcation point microphase separation at two different length scales is possible; e.g., for $n_t > 10$ values of m can be selected for which microphase separation occurs at either length scale. There is a range of (n_t, m) values for which $\Gamma_2(q)$ has two minima. Figure 5 is a projection of the above-mentioned boundary lines onto the (n_t, m) plane summarizing this behavior.

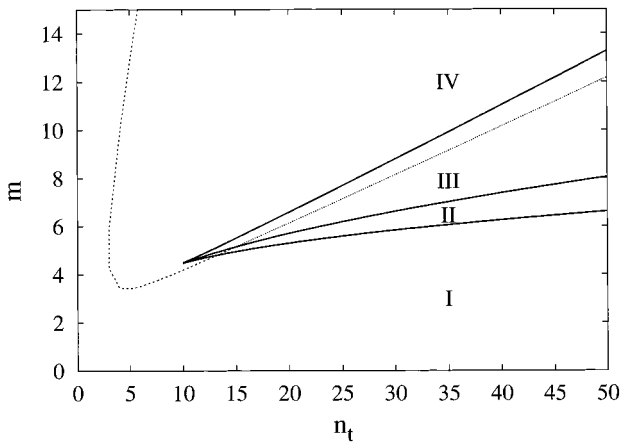

Figure 5. Classification diagram of the class of comb−coil diblock copolymer melts defined in the text. The solid lines correspond to the projections of the boundary lines in Figures 3 and 4 onto the (n_t, m) plane. Region I: Γ_2 has one minimum corresponding to the short length scale. Region II: Γ_2 has two minima; the absolute minimum corresponds to the short length scale. Region III: Γ_2 has two minima; the absolute minimum corresponds to the large length scale. Region IV: Γ_2 has one minimum corresponding to the large length scale. The dashed and dotted line presents the critical points. Inside region III, indicated with the dotted part, the critical points correspond to the relative rather than absolute minima of $\Gamma_2(q)$.

Notice that, as already observed before,[11,13] a pure comb copolymer melt essentially microphase separates on the length scale of *its* repeat unit. Therefore, the total number of monomers of the comb copolymer N must be divided by n_t in order to correctly account for the length of the repeat unit. This fact explains why the spinodal surface of Figure 3, corresponding to the short length scale (microphase separation within the comb copolymer block; Figure 2), increases linearly with n_t. On the other hand, the spinodal surface corresponding to the long length scale (large value of m) remains essentially "constant" with changing n_t. The number of monomers involved in the short length scale is N/n_t, which for the long length scale is N.

B. Critical Points. We consider the specific class of comb−coil diblock copolymers, characterized by side chains of a length equal to the length of the backbone between consecutive side chains. Therefore, an increase in f_A corresponds to an increase in the length of the homopolymer block. Because of this, critical points will only be found for special values of n_t and $m(f_A)$. In Figure 5 these critical points are presented by the dashed and dotted line. The curve has two branches, an upper and a lower branch. The upper branch is associated with the large length scale structure, i.e., the diblock scale separation. The lower branch corresponds to the short length scale, i.e., separation within the comb block. The part of the lower branch located inside region III, indicated by the dotted line, does not correspond to true critical points anymore. In region III the absolute minimum corresponds to the large length scale. The critical points correspond to the relative minimum of Γ_2. For the position of the absolute minimum of Γ_2, Γ_3 does not become zero.

For n_t values ranging from 3 to 15, critical points are present for two values of m. For $n_t > 15$, the critical point corresponding to the short length scale ordering

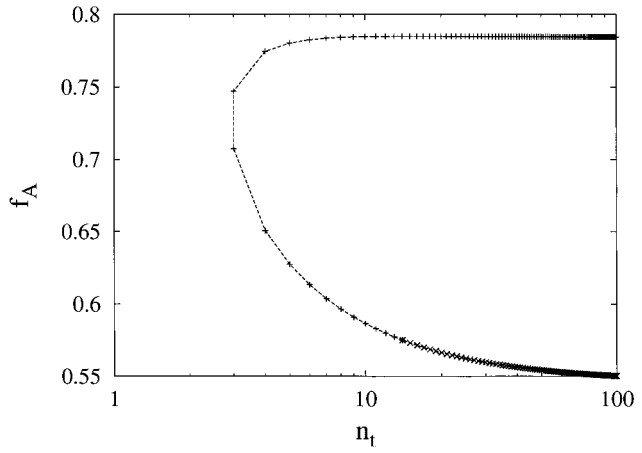

Figure 6. Critical points for comb−coil diblock copolymers. The part of its lower branch indicated with crosses ($n_t > 15$) denote the "critical points" located in region III; see also Figure 5.

no longer corresponds to the absolute minimum of $\Gamma_2(q)$. In contrast, for $n_t = 2$ there is no critical point at all. Of course, this is simply due to the specific choice of parameters. We selected $N_B = N_A^b/n_t = d$, $\alpha = 1$, and $t = 0$, and for $n_t = 2$ the critical point is located outside this particular subset of parameters.

In Figure 6, the critical points of the comb−coil diblock copolymer melt are presented once more—this time in the (n_t, f_A) plane. This presentation is better suited to show the upper branch corresponding to the critical points of the large length scale structure formation. It clearly illustrates the presence of two critical points (two values of m) for $n_t > 2$. Of course, for $n_t > 15$, the lower branch corresponds again to "pseudo"-critical points.

C. Phase Diagrams. As became clear from the spinodal analysis, the phase behavior of comb−coil diblock copolymers will be much richer. One way of presenting a phase diagram for this class of systems is to fix n_t and vary m. In this way we start with a pure comb copolymer $m = 0$ and end with nearly pure homopolymer $m \gg 1$. However, the existence of a bifurcation point in parameter space separating two distinct regions complicates matters. If we start with $n_t > 10$, the second-order vertex function will develop two minima on increasing m. First the absolute minimum will correspond to the short length scale ordering, then the two minima will attain the same value for some specific value of m, then the absolute minimum will correspond to the large length scale, and, finally, the minimum belonging to the short length scale will gradually disappear. As presented in the Theory section, the analysis of the stability of various ordered structures in block copolymer melts is usually based on a free energy expansion using a single dominant wave vector q^*, where q^* coincides with the q value for which the second order vertex function attains its minimum. So, it is quite obvious that the analysis of the microphase-separated morphology in the case where the second order vertex function has two minima of nearly equal value requires a completely different analysis involving the q values of both minima. (See ref 31.) Here we will restrict ourselves to the region in the classification diagram left of the bifurcation point where there is always only one minimum and the theory (WSL) outlined before can be applied without any restriction.

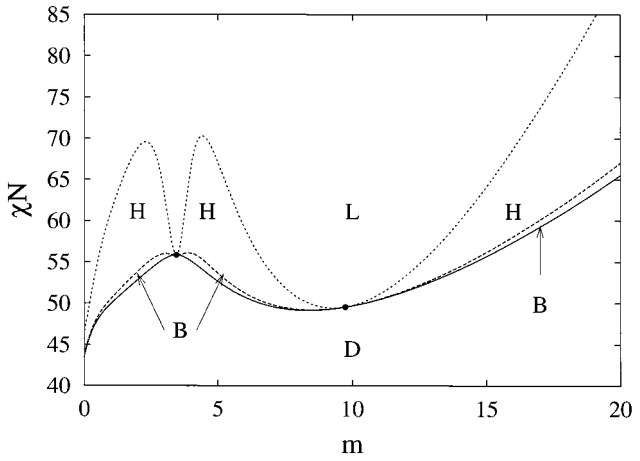

Figure 7. Phase diagram for the class of comb−coil diblock copolymer melts defined in the text. Figure corresponds to molecules with the comb block having four branch points $n_t = 4$, asymmetry parameter $t = 0$, and one side chain per branch point $\alpha = 1$ (A_m-*b*-(A-*g*-$B)_4$). Dots indicate critical points. D = disordered, L = lamellar, H = hexagonal, and B = bcc.

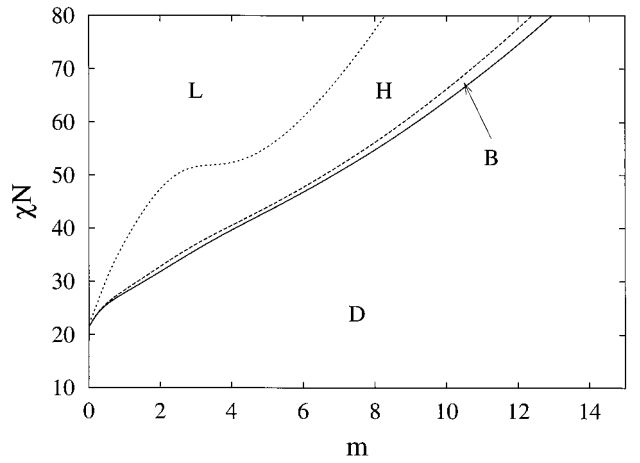

Figure 8. Phase diagram for the class of comb−coil diblock copolymer melts defined in the text. The figure corresponds to molecules with a comb block characterized by two branch points $n_t = 2$, asymmetry parameter $t = 0$, and one side chain per branch point $\alpha = 1$. Note that m corresponds to the length of the homopolymer block (A_m-*b*-(A-*g*-$B)_2$). D = disordered, L = lamellar, H = hexagonal, and B = bcc.

The phase diagrams that are presented correspond to a fixed number of branch points (n_t) and varying length of the homopolymer block (m), i.e., to slices in the (n_t, m) plane for fixed n_t. Figures 8 and 7 correspond to $n_t = 2$ and $n_t = 4$, respectively. The phase diagrams are presented as χN vs m.

For $n_t = 4$ the phase diagram has two critical points. The critical point on the left signals the change from ordering on the short (comb) length scale to ordering on the long (diblock) length scale, Figure 4. The critical point on the right corresponds to the critical point of the effective diblock copolymer. Throughout the phase diagram the lamellar (respectively hexagonal and spherical) structure is indicated with the same character L (respectively H and B). It should be realized, however, that the same symmetry is accompanied by strongly different periodicities in different regions of the phase diagram.

To illustrate this, we will walk through the phase diagram, Figure 8, as a function of the length m of the homopolymer block, keeping the value of χN fixed at

60 and 55. The corresponding changes in length scale can be found from Figure 4.

Let us start with $\chi N = 60$. For m sufficiently small there is a short length scale lamellar ordering, the layers being alternately rich in side chain B monomers and A monomers. Then a short length scale hexagonal structure is found with cylinders rich in side chain B monomers. Then a kind of in between "intermediate" length scale lamellar structure is formed, followed by a large length scale hexagonal structure with cylinders rich in homopolymer A monomers. Next, the sequence of structures follows the usual pattern from lamellar (layers alternately rich in homopolymer block and comb copolymer block) to hexagonal (cylinders rich in comb copolymer block) to bcc (spheres rich in comb copolymer block) to disordered.

For $\chi N = 55$, we start again with a short length scale lamellar structure (layers alternately rich in side chain B monomers and A monomers) followed with a short length scale hexagonal structure (cylinders rich in side chain B monomers). A sequence of short length scale bcc (spheres rich in B monomers), disordered state, and large length scale bcc (spheres rich in comb copolymer block) is then found. Next, the structures follow the same order as discussed above for $\chi N = 60$.

For $n_t = 2$ the phase diagram does not have any critical point. As discussed before, this is simply due to the choice of parameters. Going through the phase diagram at constant value of χN, e.g. 40, there is a much more gradual change in length scale.

V. Concluding Remarks

Phase diagram 7 seems quite characteristic of the class of comb−coil diblock copolymers considered. For sufficiently large values of χN a sequence of structures is found as a function of the homopolymer block length m. The first part involves the short length scale followed by large length scale ordered structures. This phase diagram was calculated for values of (n_t, m) to the left of the bifurcation point in the classification diagram (Figure 5). To the left of the bifurcation point there is gradual change from the short to the large length scale as a function of m. To the right of the bifurcation point a similar change from short to long length scale ordering will take place. However, on increasing m, we also traverse through the region where the second-order vertex function has two minima. On crossing the point where the minima are equal, a discontinuous change in length scale occurs. Here, for some values of n_t and m the occurrence of stable structures which give rise to two minima should be expected, e.g. HML, HPL, or still more complex. The free energy expansion should involve both wave vectors, and this is the main topic of our current research efforts. Preliminary calculations with two different length scales, thus with two amplitudes, led to relatively *large* amplitudes, thereby violating the assumption of WSL. Presumable, the higher harmonics of both length scales cannot be ignored in the free energy expansion. This suggests that the WSL may not be applicable there when two competing length scales are present (region III), and we should recourse to other theories, like e.g. SCFT.[17,18]

Acknowledgment. The authors are grateful to A. N. Morozov, Dr. M. Reenders, Dr. H. J. Angerman, Prof. Dr. S. Kuchanov, and Prof. Dr. I. Erukhimovich for helpful discussions.

Appendix: Correlation Functions

In this appendix we present in more detail the calculation of the correlation functions. The n-point chemical correlation function $g_{\alpha_1\cdots\alpha_n}(\mathbf{r}_1, \ldots, \mathbf{r}_n)$ denotes the probability that at point $\mathbf{r}_i$ a monomer of type α_i is present for $1 \le i \le n$.

$$g_{\alpha_1\cdots\alpha_n}(\mathbf{r}_1,\ldots,\mathbf{r}_n) = \frac{1}{N}\langle\hat{\rho}^s_{\alpha_1}(\mathbf{r}_1)\ldots\hat{\rho}^s_{\alpha_n}(\mathbf{r}_n)\rangle_0 \qquad \text{(A1)}$$

$$\langle\ldots\rangle_0 = \mathcal{N}\int\prod_{mi}\mathcal{D}\mathbf{R}^m_i \ldots \mathrm{e}^{-\hat{H}_0([\mathbf{R}_i{}^m])} \quad \langle 1\rangle_0 = 1 \qquad \text{(A2)}$$

In eq A1 $\hat{\rho}^s_\alpha$ denotes the concentration of a single molecule. Consequently, the probability measure of the ensemble average eq A2 is now also over one molecule only. Defining $\hat{\rho}^s_\alpha(\mathbf{r}) = \sum_i \sigma^i_\alpha \hat{\rho}^s_i(\mathbf{r})$, where $\hat{\rho}^s_i(\mathbf{r})$ is the microscopic single molecule concentration of block i of at position $\mathbf{r}$, eq A1 can be rewritten as

$$g_{\alpha_1\cdots\alpha_n}(\mathbf{r}_1,\ldots,\mathbf{r}_n) = \frac{1}{N}\sum_{i_1,\ldots,i_n}\sigma^{i_1}_\alpha\ldots\sigma^{i_n}_\alpha\langle\hat{\rho}^s_{i_1}(\mathbf{r}_1)\ldots\hat{\rho}^s_{i_n}(\mathbf{r}_n)\rangle_0 \qquad \text{(A3)}$$

$\langle\hat{\rho}^s_{i_1}(\mathbf{r}_1)\ldots\hat{\rho}^s_{i_n}(\mathbf{r}_n)\rangle_0$ has a similar meaning as $\langle\hat{\rho}^s_{\alpha_1}(\mathbf{r}_1)\ldots\hat{\rho}^s_{\alpha_n}(\mathbf{r}_n)\rangle_0$; it is the probability of finding a monomers of block i at position $\mathbf{r}_i$, for $1 \le i \le n$.

The correlation functions are related to the vertex functions $\Gamma_n(\mathbf{q}_1,\ldots,\mathbf{q}_n)$ of the Landau free energy expansion eq 7 by

$$\Gamma_2(\mathbf{q}_1,\mathbf{q}_2) = V(\sum_{\alpha\beta} g_{\alpha\beta}(\mathbf{q}_1)\, z_\alpha(\mathbf{q}_1)\, z_\beta(\mathbf{q}_1) - 2\chi) \qquad \text{(A4)}$$

$$\Gamma_3(\mathbf{q}_1,\mathbf{q}_2,\mathbf{q}_3) = -V\sum_{\alpha\beta\gamma} g_{\alpha\beta\gamma}(\mathbf{q}_1,\mathbf{q}_2,\mathbf{q}_3)\, z_\alpha(\mathbf{q}_1)\, z_\beta(\mathbf{q}_2)\, z_\gamma(\mathbf{q}_3) \qquad \text{(A5)}$$

$$\begin{aligned}\Gamma_4(\mathbf{q}_1,\mathbf{q}_2,\mathbf{q}_3,\mathbf{q}_4) = V\sum_{\alpha\beta\gamma\delta}[&- g_{\alpha\beta\gamma\delta}(\mathbf{q}_1,\mathbf{q}_2,\mathbf{q}_3,\mathbf{q}_4) + \\ &\sum_{\mu\nu}\{g_{\alpha\beta\mu}(\mathbf{q}_1,\mathbf{q}_2,-\mathbf{q}_1-\mathbf{q}_2)g^{-1}_{\mu\nu}(\mathbf{q}_1+\mathbf{q}_2)g_{\nu\gamma\delta}(-\mathbf{q}_3-\mathbf{q}_4,\mathbf{q}_3,\\ &\mathbf{q}_4) + g_{\alpha\gamma\mu}(\mathbf{q}_1,\mathbf{q}_3,-\mathbf{q}_1-\mathbf{q}_3)g^{-1}_{\mu\nu}(\mathbf{q}_1+\mathbf{q}_3)\, g_{\nu\beta\delta}(-\mathbf{q}_2-\mathbf{q}_4,\\ &\mathbf{q}_2,\mathbf{q}_4) + g_{\alpha\delta\mu}(\mathbf{q}_1,\mathbf{q}_4,-\mathbf{q}_1-\mathbf{q}_4)\, g^{-1}_{\mu\nu}(\mathbf{q}_1+\\ &\mathbf{q}_4)\, g_{\nu\beta\gamma}(-\mathbf{q}_2-\mathbf{q}_3,\mathbf{q}_2,\mathbf{q}_3)\}]z_\alpha(\mathbf{q}_1)\, z_\beta(\mathbf{q}_2)\, z_\gamma(\mathbf{q}_3)\, z_\delta(\mathbf{q}_4)\end{aligned} \qquad \text{(A6)}$$

where $z_\alpha(\mathbf{q}) = g^{-1}_{\alpha A}(\mathbf{q}) - g^{-1}_{\alpha B}(\mathbf{q})$.

We omit the factor $1/N$ in the remaining discussion and write $G = Ng$. As the generic example, we take the number of side chains equal to two ($n_t = 2$). Schematically the molecule is pictured below

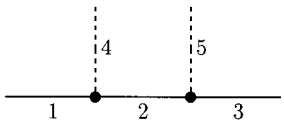

(A7)

Here $N_1 = N_2 = N_3 = N_A$ and $N_4 = N_5 = N_B$. Now we write G_{AB} in terms of G_{ij}, the block correlation functions.

$$\begin{aligned}G_{AB}(\mathbf{q}_1,\mathbf{q}_2) = G_{14}(\mathbf{q}_1,\mathbf{q}_2) + G_{15}(\mathbf{q}_1,\mathbf{q}_2) + G_{25}(\mathbf{q}_1,\mathbf{q}_2) +\\ G_{24}(\mathbf{q}_1,\mathbf{q}_2) + G_{34}(\mathbf{q}_1,\mathbf{q}_2) + G_{35}(\mathbf{q}_1,\mathbf{q}_2)\end{aligned} \qquad \text{(A8)}$$

These functions can, with the above picture in mind, be represented graphically as follows.

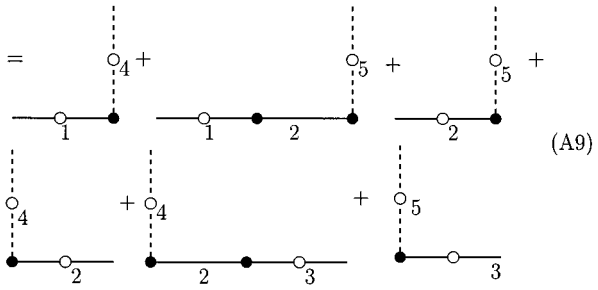

(A9)

The open dot represents the q-vector "flowing" through the block, and the solid dot denotes a branch point. The solid lines correspond to A blocks and the dashed lines to B blocks.

The calculation of G_{25} and G_{15} amounts to performing an integration over the monomers in the block, i.e., along the lines.

$$G_{25} = \int_0^{N_A}\int_0^{N_B} \mathrm{d}i\ \mathrm{d}j\ \mathrm{e}^{-x(i+j)} \tag{A10}$$

$$G_{15} = \mathrm{e}^{-xN_A} G_{25} \tag{A11}$$

Here $x = a^2q^2/6$ with $q = |\mathbf{q}_1| = |\mathbf{q}_2|$. Note that the delta function $\delta(\mathbf{q}_1 + \mathbf{q}_2)$ for momentum conservation, which arises naturally when performing the integration of eq A3, is not written down explicitly. When adding G_{25} and G_{15}, we obtain $G_{(12)5}$, the block correlation function of the combined block of blocks 1, 2, and 5. It has the same form as G_{25} only the A block is twice as long.

$$G_{(12)5} = G_{25} + G_{15} = \int_0^{2N_A}\int_0^{2N_B} \mathrm{d}i\ \mathrm{d}j\ \mathrm{e}^{-x(i+j)} \tag{A12}$$

Graphically this is represented as

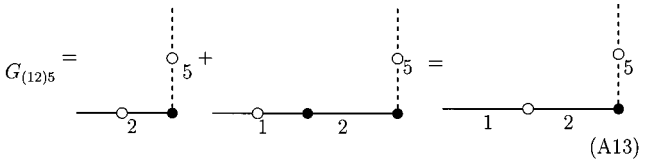

(A13)

Similarly, we contract G_{24} and G_{34} into $G_{(23)4}$ and so on. Finally, all the different diagrams of eq A8 can be contracted into "one" diagram.

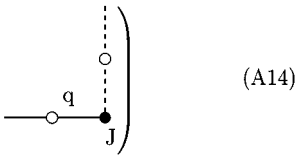

(A14)

The length of the lines is not related anymore with its length; J indicates its length. The variable J is the summation variable over the different branch points. Summation over branch points is equivalent to summing over the different lengths of all the A blocks in "front" of the side chains, i.e., in this example $J = N_A$ or $2N_A$. The prefactor 2 arises from the fact that the molecule is symmetric, thus $G_{14} = G_{35}$ and $G_{14} = G_{34}$; the backbone ends are of equal length. However, when the ends of the backbone have different lengths, they are not equal: $N_2 \neq N_{n_t+2}$. So for the comb copolymer parametrized as discussed in the Theory section ($t \neq {}^1/_2$), there will be two distinct diagrams. Note that the example molecule has no asymmetry parameter. Thus, for a comb parametrized by ($\alpha = 1$, n_t, t) the correlation function G_{AB} is

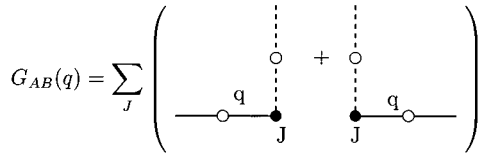

(A15)

where J runs over $\{t, t + N_A/n_t, t + 2N_A/n_t, ...\}$.

So far this method may seem rather clumsy, since the integral and subsequent summations can be done quite easily.[11] However, when we want to calculate third- and fourth-order correlation functions, this method becomes a useful bookkeeping tool and a concise way of writing down correlation functions. As an example, we present two-thirds-order correlation functions in their diagrammatic representation.

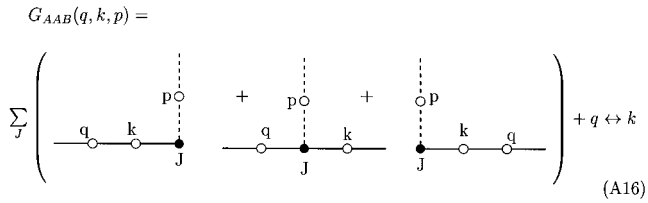

(A16)

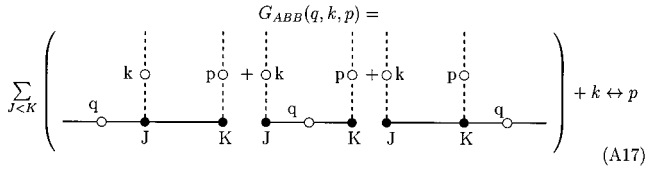

(A17)

Note that at all branch points there is momentum conservation: the momentum flowing in must be equal to the momentum flowing out. Black dots represent summation and open dots integration.

All the diagrams consist of a few elementary building blocks, e.g. lines with one, two, or more open dots and one black dot and lines between two black dots. The integrals corresponding to these building blocks can be performed in a straightforward manner. With these building blocks one can construct all the diagrams. Finally, to obtain the correlation function, one has to perform the summation. This can be done either analytically or by explicit summation. Performing the summation analytically is only feasible when the architecture is regular.

This diagrammatic representation of the correlation functions presented here is similar to the diagrammatical techniques used in particular in ref 30 (also ref 32).

References and Notes

(1) Breiner, U.; Krappe, U.; Abetz, V.; Stadler, R. *Macromol. Chem. Phys.* **1997**, *198*, 1051.
(2) Werner, A.; Fredrickson, G. H. *J. Polym. Sci., Part B: Polym. Phys.* **1997**, *35*, 849.
(3) Breiner, U.; Krappe, U.; Thomas, E. L.; Stadler, R. *Macromolecules* **1998**, *31*, 135.
(4) Ruokolainen, J.; Mäkinen, R.; Torkkeli, M.; Mäkelä, T.; Serimaa, R.; ten Brinke, G.; Ikkala, O. *Science* **1998**, *280*, 557.
(5) Ruokolainen, J.; ten Brinke, G.; Ikkala, O. *Adv. Mater.* **1999**, *11*, 777.
(6) Ruokolainen, J.; Saariaho, M.; Ikkala, O.; ten Brinke, G.; Thomas, E. L.; Torkkeli, M.; Serimaa, R. *Macromolecules* **1999**, *32*, 1152.
(7) Ott, H.; Abetz, V.; Altstädt, V. *Macromolecules* **2001**, *34*, in press.

(8) Nap, R. J.; Kok, C.; ten Brinke, G.; Kuchanov, S. I. *Eur. Phys. J. E* **2001**, *4*, 515.
(9) Beyer, F. L.; Gido, S. P.; Büschl, C.; Iatrou, H.; Uhrig, D.; Mays, J. W.; Chang, M. Y.; Garetz, B. A.; Balsara, N. P.; Beck Tan, N.; Hadjichristidis, N. *Macromolecules* **2000**, *33*, 2039.
(10) Tsoukatos, T.; Pispas, S.; Hadjichristidis, N. *Macromolecules* **2000**, *33*, 9504.
(11) Shinozaki, A.; Jasnow, D.; Balazs, A. *Macromolecules* **1994**, *27*, 2496.
(12) Foster, D. P.; Jasnow, D.; Balazs, A. C. *Macromolecules* **1995**, *28*, 3450.
(13) Benoit, H.; Hadziioannou., G. *Macromolecules* **1988**, *21*, 1449.
(14) Dobrynin, A. V.; Erukhimovich, I. Y. *Macromolecules* **1993**, *26*, 276.
(15) Olvera de la Cruz, M.; Sanchez, I. C. *Macromolecules* **1986**, *19*, 2501.
(16) Doi, M.; Edwards, S. F. In *The Theory of Polymer Dynamics*; Oxford University Press: Oxford, 1986.
(17) Hong, K. M.; Noolandi, J. J. *Macromolecules* **1981**, *14*, 727.
(18) Matsen, M. W.; Schick, M. *Phys. Rev. Lett.* **1994**, *72*, 2660.
(19) Leibler, L. *Macromolecules* **1980**, *13*, 1602.
(20) Holyst, R.; Vilgis, T. A. *Macromol. Theory Simul.* **1996**, *5*, 573.
(21) Fredrickson, G. H.; Milner, S. T.; Leibler, L. *Macromolecules* **1992**, *25*, 6341.
(22) Slot, J. J. M.; Angerman, J.; ten Brinke, G. *J. Chem. Phys.* **1998**, *109*, 8677.
(23) Mayes, A. M.; Olvera de la Cruz, M. *J. Chem. Phys.* **1989**, *91*, 7228.
(24) Olvera de la Cruz, M. *Phys. Rev. Lett.* **1991**, *67*, 85.
(25) Jones, J. L.; Olvera de la Cruz, M. *J. Chem. Phys.* **1994**, *100*, 5272.
(26) Hamley, I. W.; Bates, F. S. *J. Chem. Phys.* **1994**, *100*, 6813.
(27) Erukhimovich, I. Ya. *JETP Lett.* **1996**, *63*, 459.
(28) Milner, S. T.; Omsted, P. D. *J. Phys. II* **1997**, *7*, 249.
(29) Aksimentiev, A.; Holyst, R. *J. Chem. Phys.* **1999**, *111*, 2329.
(30) Morozov, A. N.; Fraaije, J. G. E. M. *J. Chem. Phys.* **2001**, *114*, 2452.
(31) Likhtman, A. E.; Semenov, A. N. *Macromolecules* **1998**, *31*, 9058.
(32) Read, D. J. *Macromolecules* **1998**, *31*, 899.

MA010519V